https://doi.org/10.5194/wes-2024-117
Preprint. Discussion started: 25 September 2024

eawe european academy of wind energy
Open Access WIND ENERGY SCIENCE DISCUSSIONS

IMAP-WFO: A holistic optimization tool for bottom fixed offshore wind farm design and control

Niels Roeders[1,2], Matteo Capaldo[1], Sander van Nederveen[2], and Oriol Colomés[2]

[1]TotalEnergies OneTech, Palaiseau, France
[2]Faculty of Civil Engineering and Geosciences, Delft University of Technology, Delft, The Netherlands

Correspondence: Oriol Colomés (j.o.colomesgene@tudelft.nl)

Abstract. Offshore wind farms, critical for sustainable energy production, face the challenge of optimization among many parameters influencing key performance indicators in competitive ways. This research introduces the novel Integrative Maximized Aggregated Preference Wind Farm Optimization (IMAP-WFO) framework—a comprehensive tool designed to enhance flexibility, accuracy, and uncertainty quantification in offshore wind farm design and operation. Existing methods often fall short due to limitations in adaptability and precision, especially when modeling complex multi-physical behaviors under uncertain conditions. IMAP-WFO overcomes these limitations by combining advanced statistical techniques and simulation methods. At its core are parametric design performance functions, capturing critical aspects of wind farm behavior, including energy production, material usage, and structural fatigue. These functions rely on Kriging meta-models. To address inherent uncertainty, Monte Carlo simulations provide a probabilistic assessment of outcomes. IMAP-WFO's true innovation lies in translating technical functions into socio-economic objectives, including sustainability metrics, annual energy production, capital expenditure, operational expenditure, model uncertainty, and lifetime fatigue. Stakeholders can dynamically weigh these objectives based on their preferences. A validation process ensures the accuracy of design performance functions, comparing simulated results with real-world data. IMAP-WFO's application is demonstrated through case studies: optimizing the levelized cost of energy and exploring wind farm control strategies.

1 Introduction

Offshore wind energy has emerged as a particularly promising solution for meeting renewable energy targets due to the vast potential of wind resources over open waters (Lynn). Offshore wind farms offer several advantages such as stronger and more consistent wind speeds, mitigated visual impact, and the ability to harness wind resources near densely populated coastal regions. However, the offshore environment poses unique challenges, including harsh weather conditions, logistical challenges in construction and maintenance, and economic viability. In the face of a rapidly growing global demand for renewable and

https://doi.org/10.5194/wes-2024-117
Preprint. Discussion started: 25 September 2024

eawe european academy of wind energy
Open Access WIND ENERGY SCIENCE DISCUSSIONS

sustainable energy sources, the need to increase the efficiency and competitiveness of offshore wind farms has become more critical than ever.

Optimizing a wind farm requires a holistic approach that takes into account all the different aspects involved in its development (Chen and Kim). These aspects often compete with each other when their impact is measured in terms of the Levelized Cost of Energy (LCOE). For instance, consider the distance between wind turbines. The greater the distance, the less the wake interaction (Lissaman). However, this also increases the expenditure on electrical cables. Another example is the trade-off between increasing Annual Energy Production (AEP) and the fatigue of the components. The higher the AEP, the greater the loads on the structures, and thus increased fatigue damage. This holistic approach can be ensured by implementing a multi-objective design optimization (MODO). In literature, there are already examples of MODO (Faraggiana et al.; Dykes; Kusiak and Song; Kwong et al.; Rodrigues et al.; Sorkhabi et al.; Tran et al.; van Heukelum et al.; Veeramachaneni et al.). However, those MODO strategies are often not adapted to take into account all the aspects of a wind farm development and the exploration of different operator strategies. Standard MODO approaches use monetization of the model outcomes, to compare all outcomes in the financial domain. One of the problems with monetization is that this increases uncertainty since some outcomes are hard to monetize (e.g. noise) or some outputs have a high price fluctuation (e.g. electricity production) making the model outputs less reliable. Another method is to use Pareto front optimization. This produces an infinite set of possible, supposedly equally desirable, design points (Hitoshi Furuta and Frangopol; Saad et al.) from which should be selected. However, this is inconsistent with an engineering design process where a single design optimum is desired. This makes the Pareto front method therefore of little use within the engineering design context, as also noted by those works (Lee et al.; Kim et al.). This work circumvents these shortcomings by applying a Integrative Maximised Aggregated Preference (IMAP) (van Heukelum et al.) procedure defined by MODO and operator strategies. In the IMAP MODO, all model outcomes stay in their respective domain. This is made possible through the user defining their preference for certain objective outcomes using preference functions. These preference functions act as a translation function, transferring the objective outcomes from their respective domains into a certain preference score; based on the user-defined preference function for that objective. So even though all objective outcomes can stay in their respective domains, these outcomes are later translated to a preference domain through the user-defined preference functions. This is also where the outcomes are compared and an optimum is found. This methodology is supplemented with a probabilistic description of the design performance functions, accounting for uncertainties.

This new optimization framework is named Integrative Maximized Aggregated Preference Wind Farm Optimization (IMAP-WFO), a comprehensive tool designed to enhance the flexibility, accuracy, and uncertainty quantification of offshore wind farm design and operation. This paper explores the adaptation of IMAP to offshore wind farm optimization, focusing on the strategic conflicting objectives of a single client in contrast to traditional IMAP approaches where preferences from multiple stakeholders are considered (van Heukelum et al.). A comparative case study with respect to a fictional wind farm is presented to validate the effectiveness and proof of concept of this client-centric IMAP optimization.

The paper is organized as follows: the methodology is presented in Section 2, detailing the technical design performance functions, the socio-technical objective functions, and the preference functions that translate the user's preference into the model. The results, starting from the validation of the different models considered, are presented in Section 3. Here, the case

https://doi.org/10.5194/wes-2024-117
Preprint. Discussion started: 25 September 2024

eawe european academy of wind energy
Open Access WIND ENERGY SCIENCE DISCUSSIONS

studies are presented. The first one focuses on the optimization of the layout of the wind farm and the size of the wind turbine concerning LCOE. The second case focuses on optimizing the wind farm control to show the IMAP-WFO methodology's added value. Finally, conclusions are drawn in Section 4.

2 Methodology

The IMAP-WFO model utilizes the wind turbine rotor diameter, the individual turbine spacing, and the number of standardized vessel fleets as design variables. These design variables are used in the four parametric design performance functions to represent the physical behavior of the offshore wind farm:

- Fatigue
- Energy production
- Material use
- Vessel use

These design performance functions can be tuned by the user, they can be physics-based or data-driven. In this paper, a hybrid data-driven approach based on Gaussian Process Regression (Kriging meta-models as proposed in Huchet et al.) is adapted for the first three design performance functions. The vessel use is determined through linear planning modeling. For the Kriging meta-model calibration, the reader can refer to A for details.

These design performance functions are then combined and translated into socio-technical objectives through the objective functions:

- Sustainability
- AEP
- CAPEX
- OPEX
- Wind Turbines lifetime
- Uncertainty

The user-defined preference functions guide these objective functions to represent the user-desired model output. This is done through the IMAP Genetic Algorithm that combines the objectives in the preference domain. The design performance functions act like adaptable building blocks that can be further improved and extended to enhance the model's accuracy. The design performance functions and the socio-technical objectives are detailed in the next sections. The model architecture is depicted in Figure 1. Here it can be seen that the design variables rotor diameter, turbine spacing, and the number of standardized

https://doi.org/10.5194/wes-2024-117
Preprint. Discussion started: 25 September 2024

vessel fleets combine with the boundary conditions into the parametric design performance functions. These functions are then combined into the socio-technical objectives. These objectives are controlled in the optimization by the preference functions, of which examples can be seen in Figure 2. Through these preference functions, the IMAP Genetic Algorithm can find the optimal outcomes of the design variables and the corresponding LCOE.

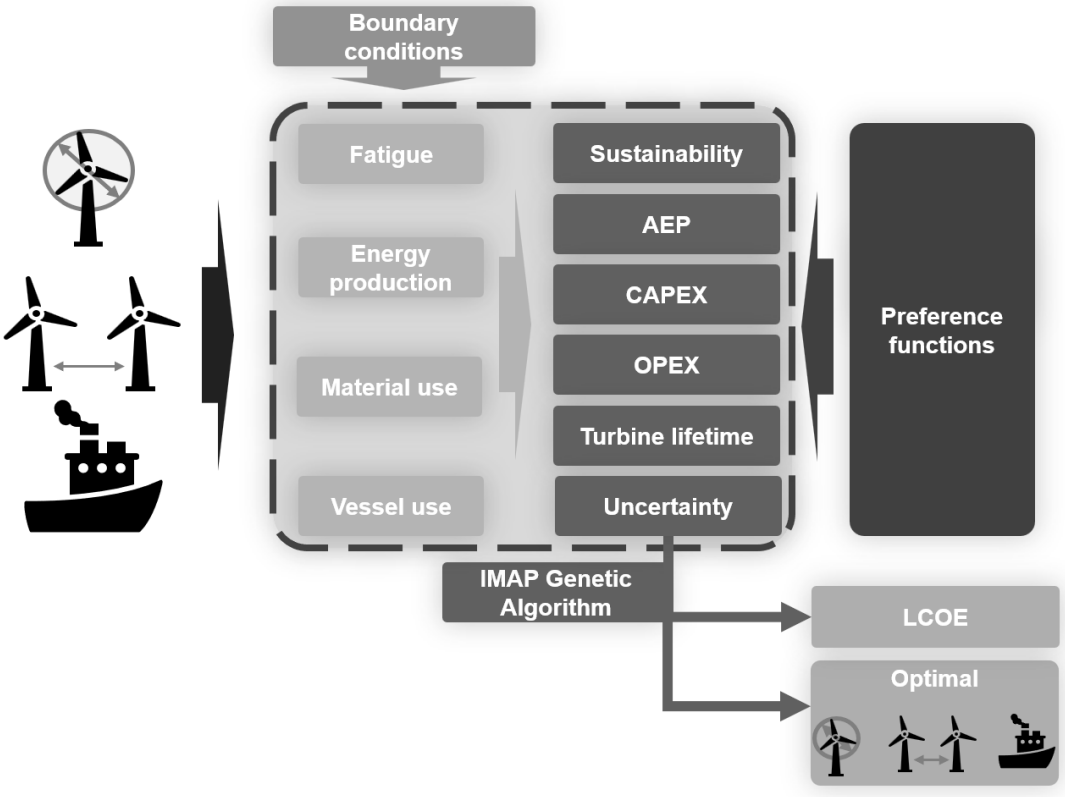

Figure 1. IMAP-WFO model architecture

2.1 Design performance functions

In this section, the design performance functions are detailed. As already observed, they can be tuned by the user, they can be physics-based or data-driven.

https://doi.org/10.5194/wes-2024-117
Preprint. Discussion started: 25 September 2024

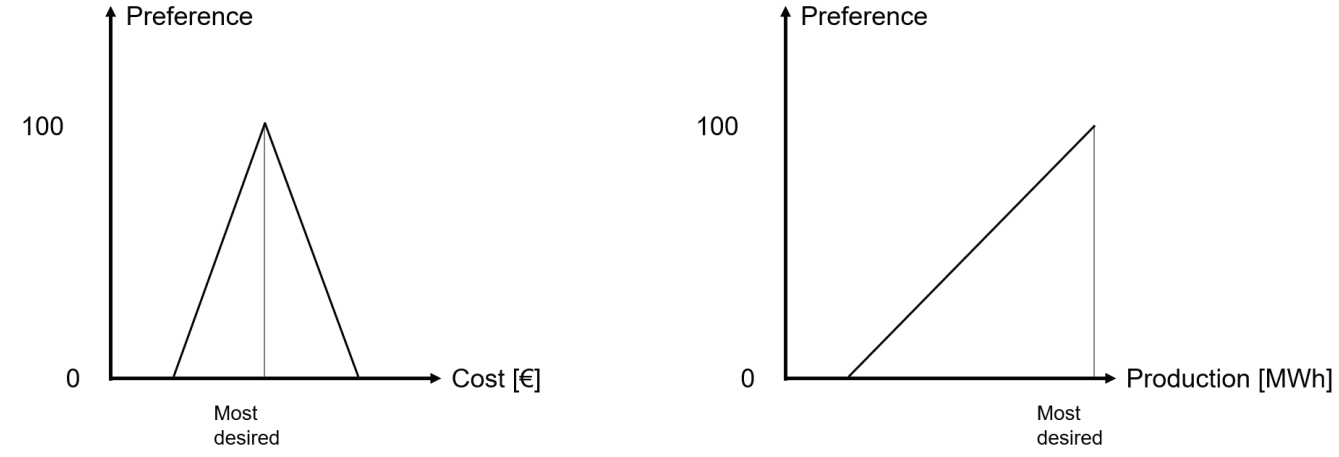

Figure 2. IMAP-WFO preference functions

2.1.1 Fatigue

The turbine fatigue is calculated through a Kriging meta-model, trained on 1296 fatigue damages that represent different load conditions for the IEA 15MW Wind Turbine calculated through the numerical model OpenFast (https://github.com/OpenFAST/openfast). These load conditions can be found in Table 1 For simplicity the number of points is limited and needs to be increased for

Table 1. The varied input variables to create a parametric surrogate model through openFAST

Variable	minimum value	maximum value	number of points
Wind speed [m/s]	3	25	4
Wind direction [°]	-90	90	3
Turbulence intensity [-]	0.0005	30	4
H_s [m]	1	11	3
T_p [s]	1	9.71	3
Wave direction [°]	-90	90	3
Current speed [m/s]	0.25	0.25	1
Current direction [°]	0	0	1

industrial applications. Moreover, for the same reason, this meta-model is used for all the design variants, meaning all the wind turbines generated by the IMAP-WFO. In future research, multiple meta-models will be used, e.g. one per wind turbine considered during the optimization.

https://doi.org/10.5194/wes-2024-117
Preprint. Discussion started: 25 September 2024

eawe european academy of wind energy
Open Access WIND ENERGY SCIENCE DISCUSSIONS

Within OpenFAST, a 60-minute simulation, with wave and wind field representing the specific environmental conditions, is performed for each load condition. From this, the tower base bending moment time series is derived and converted into fatigue damage through a rain flow counting algorithm and the Linear Damage Rule/ Miner's Rule Sutherland. The turbine spacing and rotor diameter design variables account for the added turbulence and turbine size respectively. Besides predicting the OpenFAST fatigue, the meta-model also gives the uncertainty with said prediction through the standard deviation.

2.1.2 Energy production

The energy production is calculated through PyWake Mads M. Pedersen and Réthoré (2023) with power and thrust curves, the parametric power and thrust curves proposed in Saint-Drenan et al. and Atlaskin et al., yet also made parametric for varying rated wind speed through a power and thrust curve scaling parameter. These are calculated through two Kriging meta-models, trained on 11 power and thrust curves from 3-30 MW wind turbines. With this, the power and thrust curves can be found through the rotor diameter design variable. The wind conditions are modeled through Weibull distributions, representing wind direction, wind speed, and frequency of occurrence. The turbines are placed in a grid-based layout based on the turbine spacing and rotor diameter design variables. The scaling factors, air density, and turbulence intensity are added as stochastic variables through a Monte Carlo Simulation (MCS) to account for uncertainty within these variables, and can be found in Table 2. In output, the model gives the annual energy production.

2.1.3 Material use

The material use is found through the rotor nacelle assembly (RNA), turbine tower and monopile, offshore substation, array cable, and export cable weights. The RNA and offshore substation weights are parametrically calculated by Fingersh et al.; Buchan. The tower and monopile sections are found through a Kriging meta-model, trained on high-fidelity calculated sections representing 15-22 MW wind turbines with a water depth of 30-70 meters. This is done by using a TotalEnergies in-house tool, called SeaHOWL Lataillade et al. (2024). It is assumed that the substation is located in the middle of the wind farm and that the export cable follows the shortest route from the middle to the boundary of the wind farm and then to the shore. The array cable length is found with K-means clustering, grouping the wind turbines in K clusters based on the number of turbines that can be connected to an array cable. The turbines in these clusters are connected by an array cable to the offshore substation. The total array cable length is thus represented by the length of the individual cables present in each cluster. The rotor diameter represents the rated power and the turbine spacing combined with rotor diameter represents the amount of turbines. The meta-model outcomes and air density are added as stochastic variables through an MCS to account for uncertainty within these variables and can be found in Table 2. In output, the model gives the total needed material for the wind farm.

https://doi.org/10.5194/wes-2024-117
Preprint. Discussion started: 25 September 2024

eawe european academy of wind energy
Open Access WIND ENERGY SCIENCE DISCUSSIONS

2.1.4 Vessel use

The vessel use is found through setting up linear planning for the turbine construction, cable installation, maintenance, decommissioning, and standardized fleet based on Li et al. (b). This is modeled through the linear planning module NetworkX according to the flowcharts in Figures 3, 4, 5, and 6. The turbine spacing and fleet size represent the number of turbines that need to be installed and the number of vessels for this task respectively. All activity durations from Li et al. (b) are included as stochastic variables through an MCS to account for uncertainty within these variables and can be found in Table 2. This model gives the total construction duration, decommissioning duration, vessel duration, and maintenance fleet size in output.

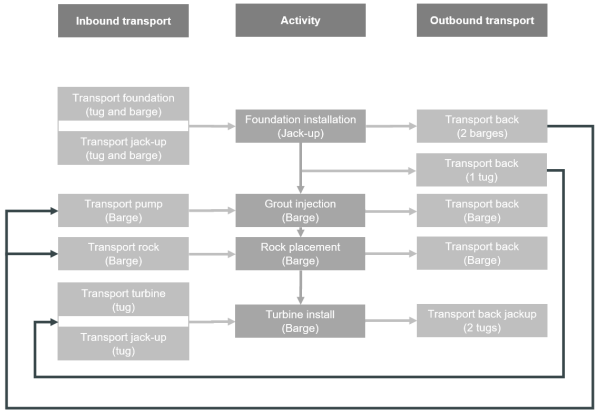

Figure 3. Flowchart turbine construction

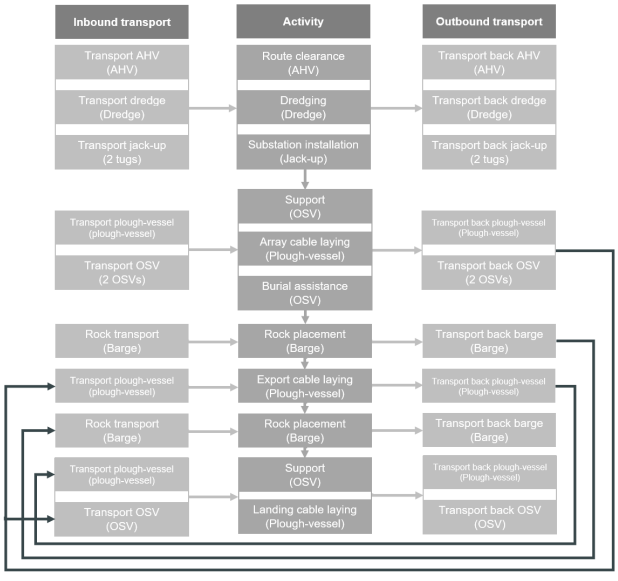

Figure 4. Flowchart cable installation

2.2 Objectives

In this section, the objective functions are detailed. Those functions cover the key performance indicators for the business model of wind farms.

2.2.1 Sustainability

The sustainability objective combines the vessel duration and the needed material from the vessel use and material use design performance function into nine sustainability scores through the Idemat eco-cost database Saravanan and Sridhar. From the needed material, the specific material types of the wind farm components are found in material composition tables. The same

https://doi.org/10.5194/wes-2024-117
Preprint. Discussion started: 25 September 2024

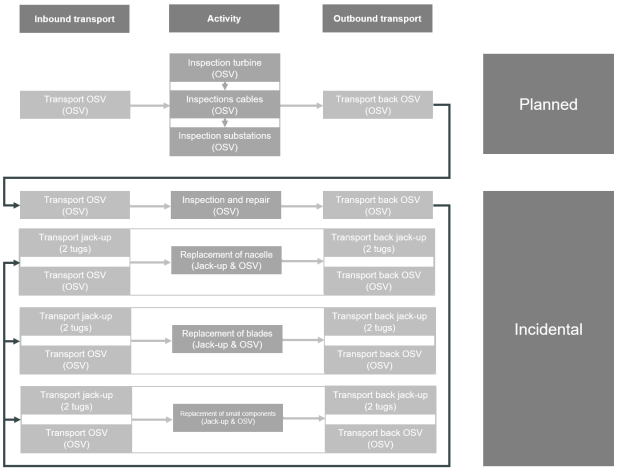

Figure 5. Flowchart maintenance

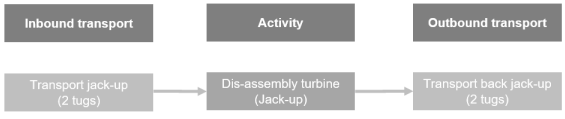

Figure 6. Flowchart decomissioning

is done for the fuel consumption from the vessel duration. These composition and consumption tables are found in Li et al. (b, a). The total sustainability score can be found on nine different scales where the output is user-defined:

1. Associated cost on human health [Euro]
2. exotoxicity [Euro]
3. Resource scarcity [Euro]
4. carbon footprint [Euro]
5. combined eco-cost [Euro]
6. ReCiPe impact human health [DALYs]
7. ReCiPe eco-toxicity [species loss/year]
8. ReCiPe resource scarcity [Euro]
9. Total carbon footprint [$kg \cdot CO_2$]

2.2.2 AED

The annual energy delivered is calculated by subtracting the yearly energy loss due to collection and export system cable resistance from the AEP, which is calculated through the energy production design performance function. The total energy loss is found by discretizing the array cables based on the number of turbine connections each cable has and calculating the energy

https://doi.org/10.5194/wes-2024-117
Preprint. Discussion started: 25 September 2024

eawe european academy of wind energy
Open Access WIND ENERGY SCIENCE DISCUSSIONS

Table 2. Parametric variables

Stochastic variable	**Min**	**Most-likely**	**Max**
Scaling factor power [-]	prediction(D)-SD(D)	prediction(D)	prediction(D)+SD(D)
Scaling factor thrust [-]	prediction(D)-SD(D)	prediction(D)	prediction(D)+SD(D)
Turbulence intensity [-]	0	10	25
Air density kg/m^3	1.1088	1.2240	1.3152
monopile diameter [m]	prediction(D)-SD(D)	prediction(D)	prediction(D)+SD(D)
monopile thickness [m]	prediction(D)-SD(D)	prediction(D)	prediction(D)+SD(D)
monopile length [m]	prediction(D)-SD(D)	prediction(D)	prediction(D)+SD(D)
towerbase diameter [m]	prediction(D)-SD(D)	prediction(D)	prediction(D)+SD(D)
towertop diameter [m]	prediction(D)-SD(D)	prediction(D)	prediction(D)+SD(D)
towerlength diameter [m]	prediction(D)-SD(D)	prediction(D)	prediction(D)+SD(D)
Construction of foundation [h]	18	24	36
Injection of grout [h]	18	24	36
Dumping of rock [h]	21.75	29	43.5
Assembly of wind turbine [h]	18	24	36
Substation installation [h/km]	6	8	12
Dredging [h/km]	18	24	36
Route clearance [h/km]	2.43	3.24	4.86
Array cable laying [h/km]	18	24	36
Support [h/km]	18	24	36
Burial assistance [h/km]	18	24	36
Rock placement [h/km]	1.5	2	3
Export cable laying [h/km]	2.65	3.53	5.3
Rock placement [h/km]	1.5	2	3
Landing cable laying [h/km]	1.2	1.6	2.4
Support [h/km]	3	4	6
Regular inspection turbine [h]	45	60	90
Regular inspection cables [h]	252	336	504
Regular inspection substation [h]	135	180	270
Irregular inspection and repair [h]	0.36	0.48	0.72
Replacement of nacelle or blades [h]	18	24	36
Replacement of small component [h]	0.36	0.48	0.72
Dis-assembly of turbine [h]	9	12	18

https://doi.org/10.5194/wes-2024-117
Preprint. Discussion started: 25 September 2024

eawe european academy of wind energy
Open Access WIND ENERGY SCIENCE DISCUSSIONS

loss for each discretization according to the power loss equation presented in Lerch et al.. Cable power and energy losses will thus increase over distance with more connections present on the cable. For the array cable, the total generated power is placed on the cable from the start.

2.2.3 CAPEX

The CAPEX is found by combining the vessel duration and needed material from the vessel use and material use design performance function with a financial cost model. The cost drivers and cost variables within this cost model can be found in Table 3 and 4. The cost variables can be refined by the user.

Table 3. CAPEX cost drivers and contributors

Cost driver	Main cost contributors
Development and project management	Rated power
Nacelle	Weight and electronics cost
Rotor	Weight
Tower	Weight and steel cost
Export cable	Length and export cable price
Array cable	Length and array cable price
Foundation	Weight and steel cost
Substation	Weight foundation and topside; costs steel and electronics
Installation	Duration vessels and dayrates
Decommissioning	Duration vessels and dayrates

2.2.4 OPEX

The OPEX is composed of different items related to different types of maintenance needed in a wind farm:

- regular maintenance: visual inspection, bolt loosening checks, etc.
- Irregular maintenance: components replacements related to component failure rates. This is associated to components considered replaceable like gearbox, bearings, generator, and blades.
- Exceptional maintenance: related to anomalies found on-site and affecting major components, like tower and foundation.

Figure 7 represents the three contributions to the maintenance evaluation considered in the IMPA-WFO.

The OPEX is calculated by the maintenance fleet size and number of maintenance events. The maintenance fleet size is derived through the vessel use design performance function, this is modeled based on Li et al. (b). The number of maintenance

https://doi.org/10.5194/wes-2024-117
Preprint. Discussion started: 25 September 2024

Table 4. User-defined cost variables

Variable	Cost [euro]
Steel price [euro/kg]	1.5
Export cable price [euro/m]	770
Array cable price [euro/m]	430
Electronics price [euro/kg]	11
Diesel price [euro/kg]	1.248
Heavy fuel oil price [euro/kg]	0.393
AHV rate [euro/day]	1100
OSV rate [euro/day]	3850
Barge rate [euro/day]	32000
Dredge rate [euro/day]	5300
Jack-up rate [euro/day]	90000
Plough-vessel rate [euro/day]	4900
Tug rate [euro/day]	1100

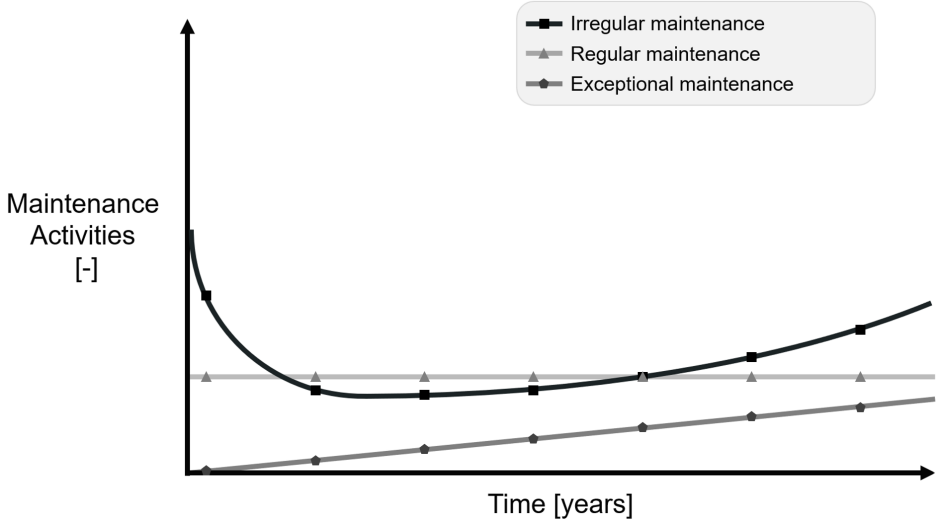

Figure 7. Contributions to OPEX

events is found through a maintenance simulator constructed on the yearly fatigue damage. In the maintenance simulator, the three contributions to the maintenance are combined: (i) the first one is constant based on regular maintenance, (ii) the second one is based on the individual component failure rate, (iii) and the third one is a monthly fatigue damage of main structure, calculated by sampling from Weibull, Jonswap and beta-PERT distributions to find windspeed, Hs, Tp and wave heading

https://doi.org/10.5194/wes-2024-117
Preprint. Discussion started: 25 September 2024

eawe european academy of wind energy
Open Access WIND ENERGY SCIENCE DISCUSSIONS

respectively. Weibull, Jonswap, and beta-PERT distributions are characterized to represent the site conditions. With this fatigue damage and failure rate, it is checked for each turbine if maintenance is necessary. The components failure rate and fatigue damage are used as a binomial probability distribution:

$$P(N) = \binom{n}{N} p^N (1-p)^{n-N}, \text{ where } \mathrm{n} = 1 \tag{1}$$

If due to this probability maintenance needs to occur for a main structure, its fatigue damage is reset to 0 due to the executed repair. If maintenance does not occur for a turbine, the new yearly fatigue damage is determined from the distributions and accumulated to the previous damage. Equivalently, if a component fails due to its failure rate, the aging of the component is reset to zero otherwise the failure probability follows the failure rate distribution per year defined by the user. This is now the new probability maintenance needs to occur this year. This process is repeated for all turbines for all years in their lifetime. This gives the total amount of needed maintenance events over the lifetime, which can be calculated back to yearly maintenance events by dividing by lifetime. A flowchart for this maintenance simulator can be found in Figure 8.

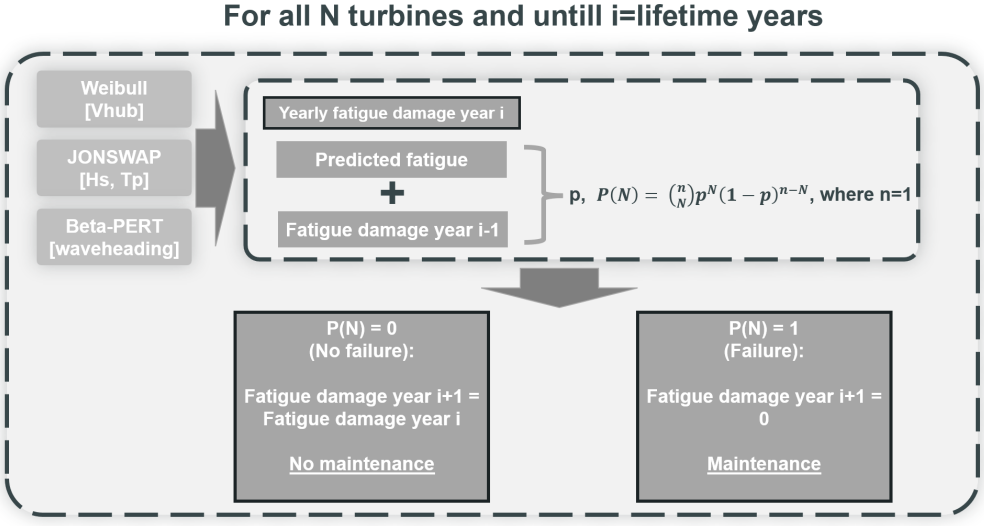

Figure 8. Maintenance simulator

2.2.5 Wind Turbine Lifetime

The lifetime fatigue damage is a technical objective function that calculates the operational lifetime by considering the fatigue of wind turbines over their entire lifetime, without incorporating any economic components. It operates similarly to the OPEX maintenance simulator, but focuses solely on fatigue, continuously increasing to account for lifetime fatigue without utilizing binomial simulation.

https://doi.org/10.5194/wes-2024-117
Preprint. Discussion started: 25 September 2024

eawe european academy of wind energy
Open Access WIND ENERGY SCIENCE DISCUSSIONS

On the other hand, the fatigue meta-model uncertainty assesses the degree of uncertainty in the fatigue meta-model for specific variants, which refers to the variability or confidence level in the predictions. This uncertainty is quantified as the coefficient of variation (standard deviation/mean), providing a measure of how much the actual fatigue might differ from the predicted values, with accuracy represented on a scale from 0 (most accurate) to 1 (least accurate).

2.3 Preference functions

Preference functions connect the user preference to the objective functions. van Heukelum et al. describes the basic theory behind preference function modeling and how to set up a preference curve. Only linear and triangular preference curves have been used in this research.

2.4 IMAP Genetic Algorithm

For the IMAP methodology, a modified Genetic Algorithm is created in van Heukelum et al. with the novel addition of preference aggregation. The adapted Genetic Algorithm works like a regular GA with the important difference that before evaluation, all the individual objective outcomes are coupled to their respective preference curves. After this, the population members will have a preference score for each objective separately. Based on the objective weights, these are then aggregated to give a preference score for the population members. From this, the Genetic Algorithm continues as usual, now identifying the best preference scores. Figure 9 gives a schematic representation of a single population iteration of this IMAP GA.

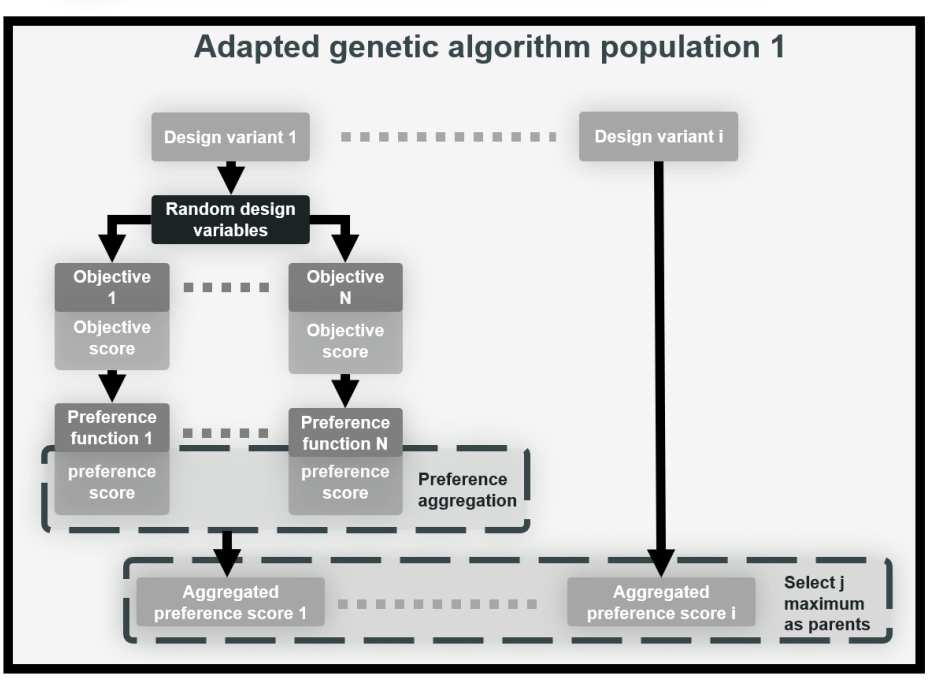

Figure 9. IMAP GA

https://doi.org/10.5194/wes-2024-117
Preprint. Discussion started: 25 September 2024

eawe european academy of wind energy
Open Access WIND ENERGY SCIENCE DISCUSSIONS

3 Results

3.1 Validation of the models

The quality and accuracy of the generated data from the design performance functions are tested by using reference projects to which the model outputs can be compared.

3.1.1 Fatigue

A comparison is made between the fatigue calculation of an existing turbine in a wind farm and the outcome of the fatigue calculated through the Kriging meta-model trained on OpenFAST data. The outcome of the real-case and the proposed meta-model calculation both stay under the critical value for lifetime fatigue.

3.1.2 Energy production

For the validation of the energy production, the power and thrust curves and the total AEP are compared to a reference wind farm in the North Sea. From this, it is found that the model power curve slightly underestimates the total power due to increased turbulence assumptions and a more conservative cut-out speed. These power and thrust curve comparisons can be seen in Figure 10. Due to this, the total AEP shows a slight underestimation of the fatigue of 6.4%.

3.1.3 Material use

The material use for the foundations and the array cables are investigated since these are the two main contributors that represent the characteristics of the wind farm. Firstly, the material use for the foundations is directly correlated to the rated power of a turbine due to the weight the foundation has to withstand. Since the monopile sections are determined by a Kriging meta-model trained on high-fidelity calculated sections, this material use is highly accurate for turbines of 15-22MW with a water depth of 30-70 meters.

Secondly, the material use for the array cables is directly proportionate to the turbines' rated power, their placement within the wind farm, and the wind farm size. The array cable length is calculated through a simplified K-means clustering method which gives an overestimation of 74% of the cable weight. This overestimation can be mitigated by adapting the cable price in 4.

3.1.4 Vessel use

To validate the vessel use, the calculated construction and decommissioning duration is compared to the actual construction and planned decommissioning duration of an existing wind farm. For the calculation, the standardized fleet based on Li et al.

https://doi.org/10.5194/wes-2024-117
Preprint. Discussion started: 25 September 2024

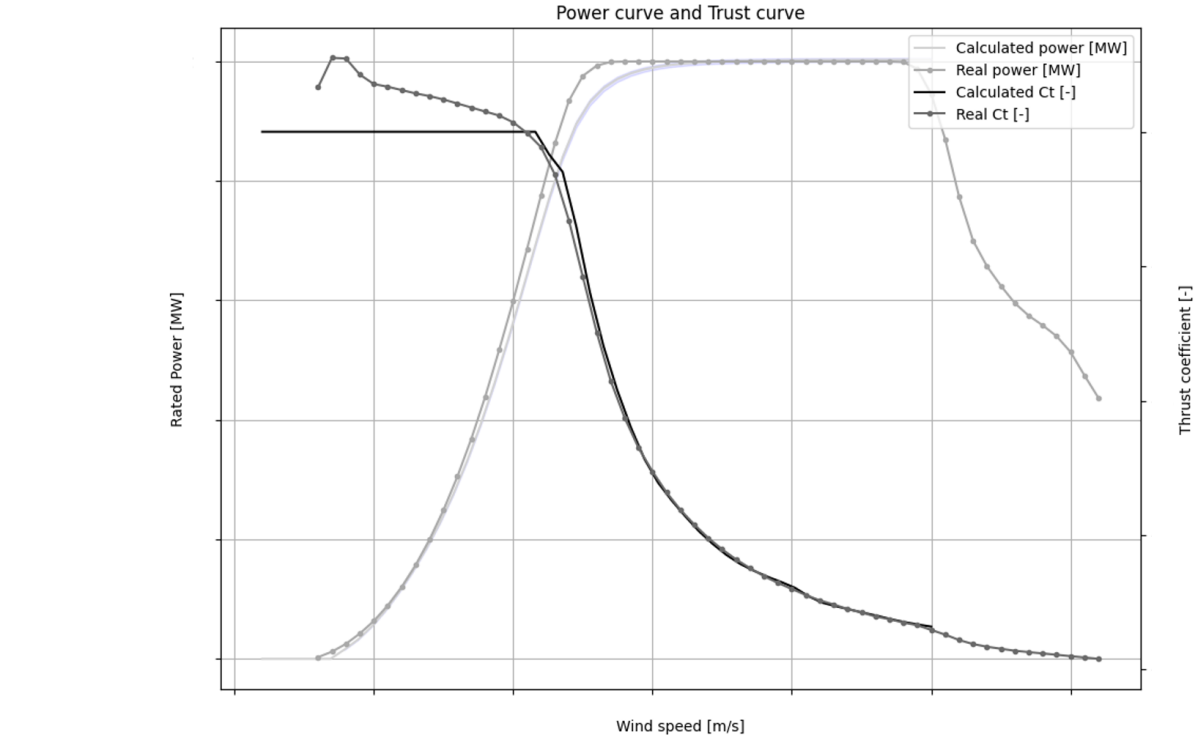

Figure 10. Comparison modeled and real power and thrust curves

(b) is used. From this, a construction duration of two years and a decommissioning period of one year is found, which is the same as the actual and planned construction and decommissioning periods.

3.2 Global model settings

For the two result cases, the settings of the model are summarized in Table 5

Both cases will be set up following the boundary conditions of an existing TotalEnergies wind farm in the North Sea, with typical environmental conditions. Due to confidentiality, specifics can not be disclosed. Because of insufficient supplier information, irregular maintenance has been excluded for now.

3.3 Case study 1: design for optimal LCOE

The goal of this case is to show the capability of IMAP-WFO to compete with existing models by finding the design that creates the minimum LCOE for a reference wind farm location and constraints. This is done by creating an additional objective function for the LCOE based on 2.

https://doi.org/10.5194/wes-2024-117
Preprint. Discussion started: 25 September 2024

eawe european academy of wind energy
Open Access WIND ENERGY SCIENCE DISCUSSIONS

Table 5. Used standard setting to create results model

Setting	Used option
Cable current [A]	800
Water depth [m]	50
Array cable voltage [kV]	66
Export cable voltage [kV]	132
Lifetime [years]	25
Sustainability scale [-]	ReCiPe human health
N Monte Carlo [-]	10
Material prices/day rates [euro]	see Table 4
Tower and monopile dimensioning method	Meta-model
Array cable calculation	K-means
GA population [-]	100
GA convergence criteria	N_{stall} = 5

$$\text{LCOE} = \frac{(\text{CAPEX} * \text{FCR}) + (\text{OPEX} * T_{lifetime})}{\text{AEP} * T_{lifetime}} \tag{2}$$

Here, the FCR is set to $1/T_{lifetime}$ which ensures a break-even LCOE at the end of a lifetime. With this new objective function, an optimization can be performed for just the LCOE when this objective is given the weight of 1. The preference function has 100 preference at an LCOE of 0 euros and 0 preference at an LCOE of 250 euros/MWh (the assumed maximum bound). These adjustments adapt the MODO model into a traditional SODO model that minimizes LCOE. The design variable ranges used for optimization can be found in Table 6.

Table 6. Bounds design variables minimization LCOE

Design variable	Lower bound	Upper bound
Turbine spacing [Turbine diameters]	6	13
Rotor diameter [m]	90	340
fleet size [-]	1	10

The minimized LCOE comes down to 25.43 €/MWh, for an amount of 12 turbines with a diameter of 314 meters, individual spacing of 6.2 diameters, and 3 fleets for construction. The optimal solution corresponds to a 25 MW turbine. These large turbines are not already in the market but the industry is projecting to have those size in the roadmap to be developed in the coming years. This implies that the largest turbines are not necessarily economically optimal since the optimization converged

https://doi.org/10.5194/wes-2024-117
Preprint. Discussion started: 25 September 2024

towards a diameter of 314 meters instead of the limit of 340 meters. However, it is clear that the minimal LCOE is found through larger turbines than the ones used nowadays. This LCOE is lower than found in literature noa on reference projects, which can be explained since this turbine size is not yet feasible at present and the fact that the model does not account for the technical, supply chain, and construction hurdles that come into play for these very large wind turbines. However, the optimization workflow works properly and, for the considered design performance functions and the objective functions, the LCOE is minimized. Small variation around the solution have been tested in order to assess the minimum, indeed.

Figure 11 shows the AEP, CAPEX, and OPEX preference curves and the wind farm layout that corresponds to this optimal design.

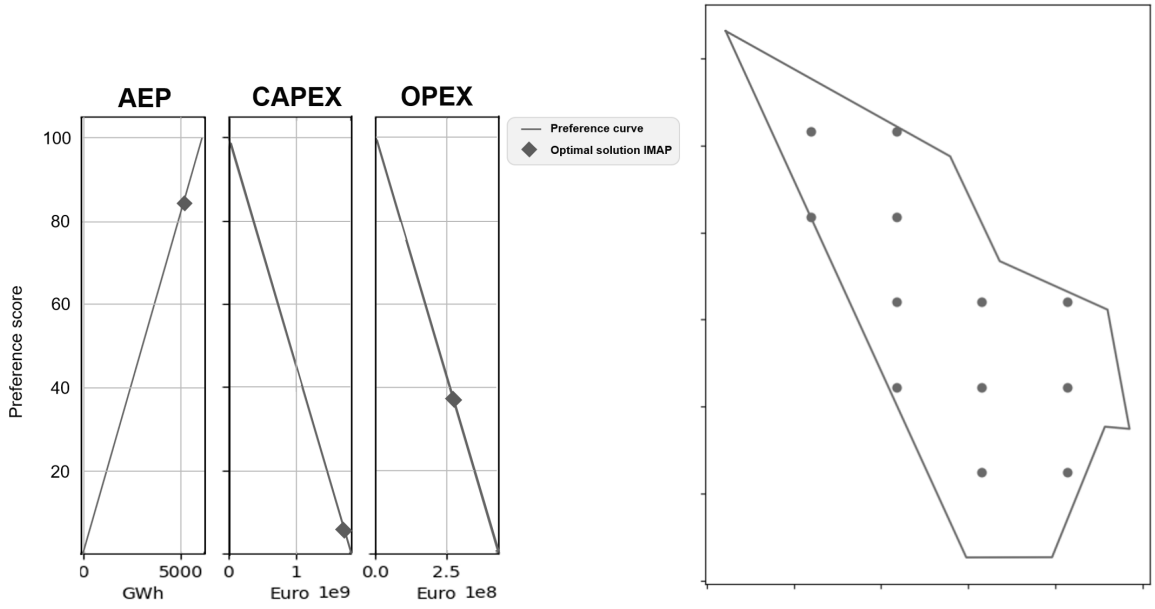

Figure 11. Preference cures AEP, CAPEX, and OPEX and layout for optimal windfarm

It can be seen that AEP has a high individual preference score of 84. CAPEX has a lower preference score of 4.6 and OPEX again has a high individual score of 38.9. The maximum x-value of these objectives represents the maximum value possible for these objectives within the design variable ranges (Table 6). Within these ranges, the optimum AEP has a preference of 84 when compared to all the other possible AEP variants. From this, the individual weights of AEP, CAPEX, and OPEX can be calculated to be 0.65, 0.04, and 0.30 respectively by normalizing the preference scores. This shows the influence of these three objectives on the minimized LCOE through an IMAP approach. This implies that the order of decreasing influence for these KPIs is AEP, OPEX, and CAPEX. This can be explained by the fact that the LCOE is calculated for an FCR that represents financial break-even at the end of the lifetime. If a higher FCR, thus higher profitability, is chosen, the significance of CAPEX on the LCOE would increase at the cost of OPEX and AEP. The importance of CAPEX is thus dependent on FCR.

https://doi.org/10.5194/wes-2024-117
Preprint. Discussion started: 25 September 2024

eawe european academy of wind energy
Open Access WIND ENERGY SCIENCE DISCUSSIONS

3.4 Case study 2: Optimized wind farm control

The goal of the second case is to prove the added value of the proposed optimization framework by illustrating the versatility of the application of the IMAP-WFO methodology. Here, it is investigated how many turbines of a predefined wind farm should be used for production to find the amount of energy that is desired, while at the same time minimizing turbine tower lifetime fatigue due to bending moments. This is done for energy prices between 75 and 250 €/MWh. In other words, in this use case, the wind farm is controlled by taking into account the energy price and optimising the fatigue by keeping the same revenue.

However, in this way, the control is completely dependent on the energy price. In reality, there will be a certain minimum production set up with the energy consumer. This implies that the proposed control scenario is not applicable until this minimal production is met. Everything above this minimum could be controlled as described in this use case.

First, the model outcome for CAPEX and OPEX are found for the existing wind farm by setting the design variables to the values of the predefined wind farm. They stay constant. Then, the rotor diameter design variable is fixed at 164 meters (a common current size) and the inter-turbine spacing is made parametric. This allows the spacing to become larger than the original, which places fewer turbines in the same area. From this, the total amount and location of the turbines that should be used for a scenario can be found.

To couple the energy price to the optimization process, Equation 3 is used to find the AEP based on CAPEX, yearly return on initial investment, OPEX, and energy price. For this case, the ROI is chosen as the breakeven point in the lifespan ($1/T_{lifetime}\%$).

$$\text{AEP} = \frac{(\text{CAPEX} * \text{ROI}) + \text{OPEX}}{\text{LCOE (energy price)}} \tag{3}$$

The AEP value is implemented in the optimization as a constraint modeled as a triangular function through the preference function, as illustrated in Figure 12. This function has the desired AEP as a 100 score and then sharply decreasing scores for a lower and upper bound AEP. These bounds are still defined since they give the optimization algorithm the chance to improve on the different design variants found. The optimization has been performed for seven different energy prices between 75-250

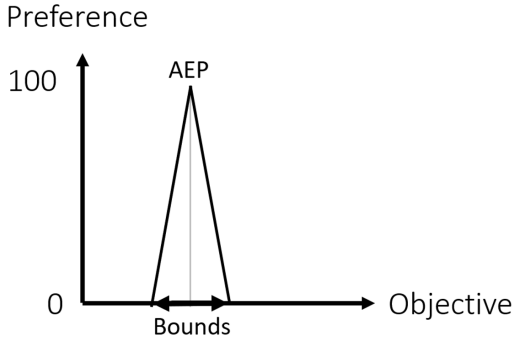

Figure 12. AEP preference function

https://doi.org/10.5194/wes-2024-117
Preprint. Discussion started: 25 September 2024

eawe european academy of wind energy
Open Access WIND ENERGY SCIENCE DISCUSSIONS

300 €/MWh, from which the number of turbines that should be used for production can be seen in Table 7 and Figure 13. It can be seen that the revenue (product of Energy price and AEP) is kept constant during the optimization of the wind farm control.

Table 7. Windfarm control results

Energy price (€/MWh)	AEP (MWh)	Producing turbines [-]	Rate of decrease [%]	Global change[%]
75	654	15	100	100
94	523	12	80	80
112.5	435	10	83	67
131.3	373	9	90	60
150	327	7	78	47
200	245	6	86	40
250	196	5	83	33

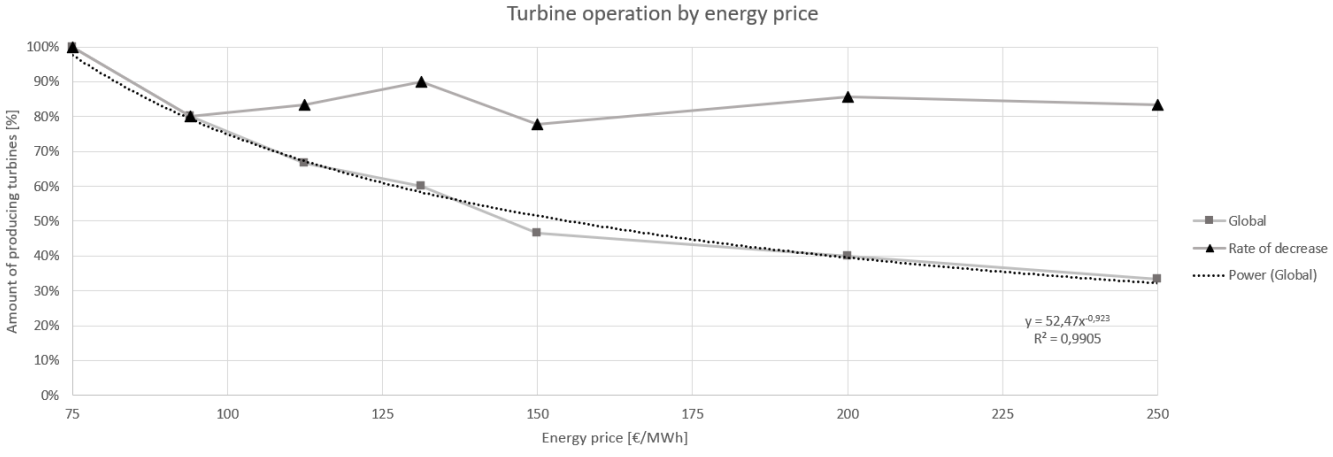

Figure 13. Turbine operation by energy price graph

Figure 15 gives the control scheme for the reference wind farm. Here, grey shows producing, and black shows non-producing wind turbines over the different energy price scenarios.

The largest difference in the amount of producing turbines takes place from 75 to 94 €/MWh, where 20% of the turbines 305 can be taken out of production. At the maximum investigated energy price of 250 €/MWh, 67% of the turbines can be taken out of production.

https://doi.org/10.5194/wes-2024-117
Preprint. Discussion started: 25 September 2024

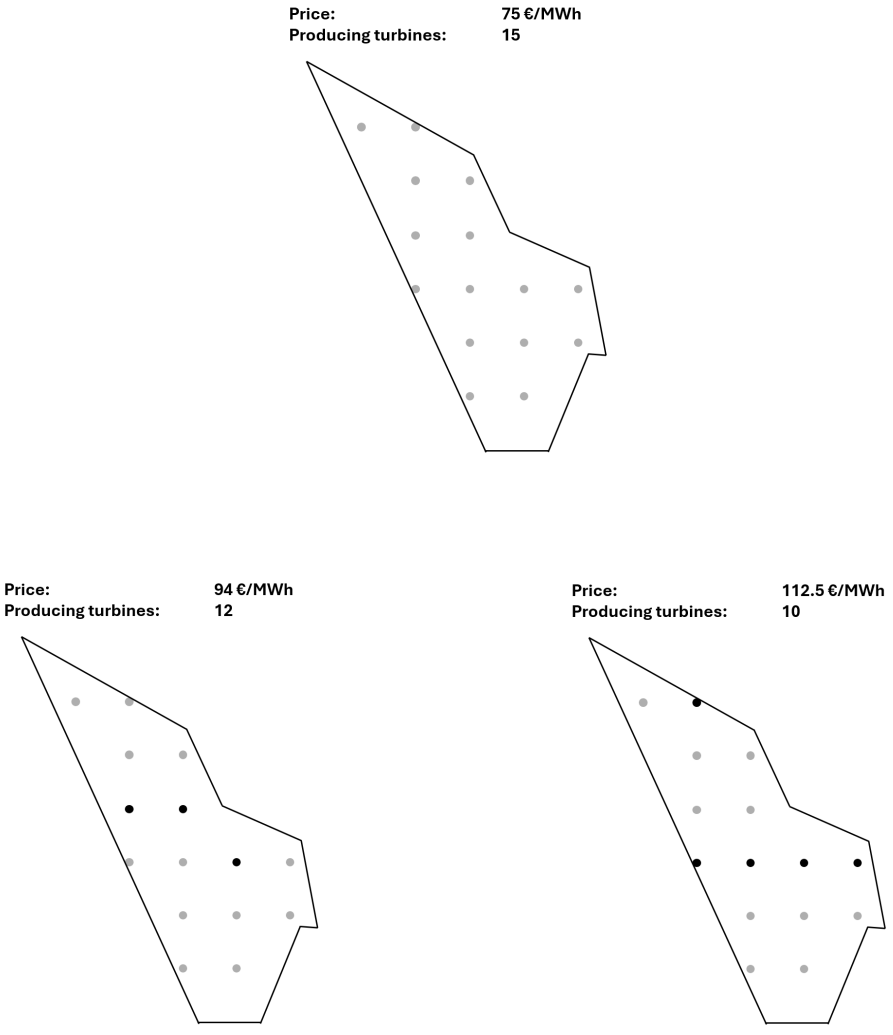

Figure 14. Wind farm control scheme for different energy prices: 75 €/MWh, 94 €/MWh and 112.5 €/MWh.

Besides, the control scheme prescribes a static measure for a certain energy price. If the energy price stays steady for an extended period, this will thus stress the turbines that are active for this control scheme. In this case, a more adaptive strategy would need to take place to keep decreasing fatigue for these turbines.

In the future, to make it more industrial feasible, the use case will be improved by considering a de-rating of the wind turbines and not the complete shut down of them.

https://doi.org/10.5194/wes-2024-117
Preprint. Discussion started: 25 September 2024

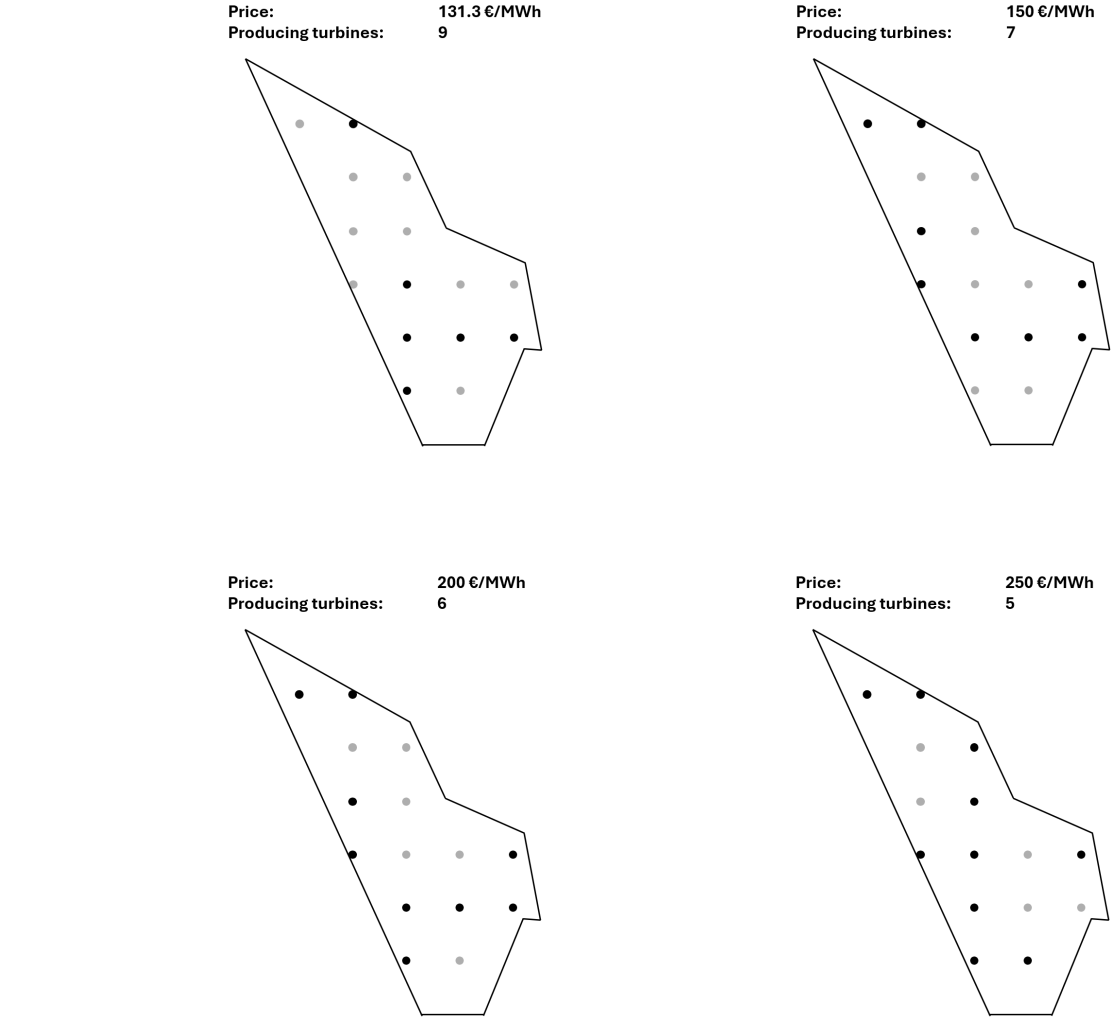

Figure 15. Wind farm control scheme for different energy prices: 131.3 €/MWh, 150 €/MWh, 200 €/MWh and 250 €/MWh.

4 Conclusions

This work presents a new method named the probabilistic Integrative Maximised Aggregated Preference Wind Farm Optimization approach (IMAP-WFO). This optimization tool aims at making offshore wind farms more efficient and cost-effective. This method uses Kriging meta-models to build functions that predict how a wind farm will perform. These functions cover energy production, material usage, vessel usage, and fatigue. These functions are tested using Monte Carlo simulations to understand the accuracy and possible limitations of their predictions. These design performance functions are then combined and translated into socio-technical objectives through the objective functions (key parameter functions of a wind farm). The user-defined pref-

https://doi.org/10.5194/wes-2024-117
Preprint. Discussion started: 25 September 2024

erence functions guide these objective functions during the optimization (by genetic algorithm) to represent the user-desired model output.

The IMAP-WFO model was utilized in two main scenarios. The first scenario aimed to see if the model could do better than existing ones by trying to lower the Levelized Cost of Energy (LCOE). The model suggested a wind farm setup that significantly lowered the LCOE to 25.43 €/MWh, which is the minimum by considering those design performance functions. It showed that the model converges to larger turbines, which are expected to be developed in the coming years, while also pointing out that bigger turbines aren't always the best option.

In the second scenario, we looked at how to control the wind farm to reduce loading on the turbines over time, considering different electricity price scenarios for production. The model identified ways to adjust which turbines are running to extend their useful life and manage costs better, depending on electricity prices. The revenue is kept constant. This approach could help reduce maintenance costs, increase lifetime, and make the wind farm more profitable.

The results from these scenarios prove that the IMAP-WFO model is a strong tool for designing and controlling offshore wind farms. It's flexible in meeting different goals and good at dealing with uncertainties and complex behaviors. The findings can help the wind energy industry build and operate wind farms in a more sustainable, efficient, and cost-effective way.

Moving forward, there are several ways to make the IMAP-WFO model even better, such as improving how it calculates cable lengths, adding more detail to the models predicting fatigue, running more simulations to get more accurate predictions, including irregular maintenance, and refining the main models used. Additionally, future research could explore how different financial strategies affect costs, how much fatigue can be reduced through this methodology, how agreements on minimum electricity production can be included in the model, explore flexible ways to manage the wind farm, and perform a sensitivity analysis on the settings of the optimization algorithm.

Appendix A: Kriging meta-model calibration

For supervised data-driven meta-modeling, the meta-model needs to be trained on the data it is supposed to predict. This is achieved using the right covariance matrix and by finding the correct hyperparameters, which is done through the following steps.

- **Hyperparameter Estimation**: Once the autocorrelation model is specified, the next step is to estimate the hyperparameters. These are parameters that govern the behavior of the autocorrelation function and, by extension, the kriging model itself. The estimation is performed using the available dataset. This first estimation will form the starting point for finding the actual hyperparameters.

- **Training and Validation Set Creation**: A subset of the full dataset is randomly selected to form the training and validation sets. The proportion of data allocated to training is predetermined by a set training percentage. The training set is used to build the model, while the validation set is reserved for testing its predictive accuracy.

https://doi.org/10.5194/wes-2024-117
Preprint. Discussion started: 25 September 2024

eawe european academy of wind energy
Open Access WIND ENERGY SCIENCE DISCUSSIONS

- **Meta-Model Setup and Calibration**: The meta-model is configured based on the training dataset. Calibration is then achieved by comparing the meta-model's predictions against the observed values in the validation dataset. This comparison is quantified using the Mean Squared Error (MSE), which measures the average of the squares of the errors between predicted and observed values.

- **Hyperparameter Selection Function**: A function is defined to select the hyperparameters by returning the MSE as its output. This function encapsulates the calibration process and serves as the objective function for the subsequent optimization step.

- **Minimization Algorithm Execution**: The hyperparameter selection function is executed within a minimization algorithm. The goal of this algorithm is to find the set of hyperparameters that result in the minimal MSE. The hyperparameters that achieve this are deemed the most accurate and are denoted by θ

- **Final Meta-Model Creation**: With the optimal hyperparameters θ identified, the final meta-model is constructed for the complete dataset. This model is expected to have reliable predictive capabilities due to the calibration process it has undergone.

In this study, the squared exponential function has been chosen as covariance matrix due to its anisotropic behavior and high smoothness which is crucial for accurate multi-dimensional predictions.

Author contributions. **Niels Roeders:** Conceptualization, Methodology, Software, Validation, Investigation, Writing - Original Draft; **Matteo Capaldo:** Conceptualization, Methodology, Supervision, Writing - Original Draft; **Sander van Nederveen:** Conceptualization, Methodology, Supervision, Writing - Original Draft; **Oriol Colomés:** Conceptualization, Methodology, Supervision, Writing - Original Draft;

Competing interests. The authors declare that they have no known competing financial interests or personal relationships that could have appeared to influence the work reported in this paper.

https://doi.org/10.5194/wes-2024-117
Preprint. Discussion started: 25 September 2024

eawe european academy of wind energy
Open Access WIND ENERGY SCIENCE DISCUSSIONS

References

2023 Levelized Cost Of Energy+, https://www.lazard.com/research-insights/2023-levelized-cost-of-energyplus/.

Atlaskin, E., Suomi, I., and Lindfors, A.: Statistical calculation of thrust curve of a wind turbine based on available power curve and general specifications data, pp. EGU21–14 402, https://doi.org/10.5194/egusphere-egu21-14402, conference Name: EGU General Assembly Conference Abstracts ADS Bibcode: 2021EGUGA..2314402A.

Buchan, V.: Offshore Substations: Fixed or Floating? – Technoeconomic Analysis.

Chen, J. and Kim, M.-H.: Review of Recent Offshore Wind Turbine Research and Optimization Methodologies in Their Design, 10, 28, https://doi.org/10.3390/jmse10010028, number: 1 Publisher: Multidisciplinary Digital Publishing Institute.

Dykes, K.: Optimization of Wind Farm Design for Objectives Beyond LCOE, 1618, 042 039, https://doi.org/10.1088/1742-6596/1618/4/042039.

Faraggiana, E., Sirigu, M., Ghigo, A., Bracco, G., and Mattiazzo, G.: An efficient optimisation tool for floating offshore wind support structures, 8, 9104–9118, https://doi.org/10.1016/j.egyr.2022.07.036.

Fingersh, L., Hand, M., and Laxson, A.: Wind Turbine Design Cost and Scaling Model, https://doi.org/10.2172/897434.

Hitoshi Furuta, Takahiro Kameda, K. N. Y. T. and Frangopol, D. M.: Optimal bridge maintenance planning using improved multi-objective genetic algorithm, 2, 33–41, https://doi.org/10.1080/15732470500031040, publisher: Taylor & Francis _eprint: https://doi.org/10.1080/15732470500031040.

Huchet, Q., Mattrand, C., Beaurepaire, P., Relun, N., and Gayton, N.: AK-DA: An efficient method for the fatigue assessment of wind turbine structures, 22, 638–652, https://doi.org/10.1002/we.2312.

Kim, S., Frangopol, D. M., and Ge, B.: Probabilistic multi-objective optimum combined inspection and monitoring planning and decision making with updating, 18, 1487–1505, https://doi.org/10.1080/15732479.2022.2061015, publisher: Taylor & Francis _eprint: https://doi.org/10.1080/15732479.2022.2061015.

Kusiak, A. and Song, Z.: Design of wind farm layout for maximum wind energy capture, 35, 685–694, https://ideas.repec.org//a/eee/renene/v35y2010i3p685-694.html, publisher: Elsevier.

Kwong, W. Y., Zhang, P., Romero, D., Moran, J., Morgenroth, M., and Amon, C.: Multi-Objective Wind Farm Layout Optimization Considering Energy Generation and Noise Propagation With NSGA-II, 136, 1–10, https://doi.org/10.1115/DETC2012-71478.

Lataillade, T. D., Yu, W., Pallud, M., and Capaldo, M.: SEAHOWL: Partitioned Multiphysics and Multifidelity Modelling of Wind Turbines with Monolithically Coupled Elastodynamics, Journal of Physics: Conference Series, 2767, 052 051, https://doi.org/10.1088/1742-6596/2767/5/052051, 2024.

Lee, S.-Y., Park, W., Ok, S.-Y., and Koh, H.-M.: Preference-based maintenance planning for deteriorating bridges under multi-objective optimisation framework, 7, 633–644, https://doi.org/10.1080/15732479.2010.501565, publisher: Taylor & Francis _eprint: https://doi.org/10.1080/15732479.2010.501565.

Lerch, M., De-Prada-Gil, M., and Molins, C.: Collection Grid Optimization of a Floating Offshore Wind Farm Using Particle Swarm Theory, 1356, 012 012, https://doi.org/10.1088/1742-6596/1356/1/012012.

Li, C., Mogollón, J. M., Tukker, A., Dong, J., von Terzi, D., Zhang, C., and Steubing, B.: Future material requirements for global sustainable offshore wind energy development, 164, 112 603, https://doi.org/10.1016/j.rser.2022.112603, a.

Li, C., Mogollón, J. M., Tukker, A., and Steubing, B.: Environmental Impacts of Global Offshore Wind Energy Development until 2040, 56, 11 567–11 577, https://doi.org/10.1021/acs.est.2c02183, publisher: American Chemical Society, b.

https://doi.org/10.5194/wes-2024-117
Preprint. Discussion started: 25 September 2024

Lissaman, P. B. S.: Energy Effectiveness of Arbitrary Arrays of Wind Turbines, 3, 323–328, https://doi.org/10.2514/3.62441, publisher: American Institute of Aeronautics and Astronautics.

Lynn, P. A.: Onshore and Offshore Wind Energy: An Introduction, John Wiley & Sons, ISBN 978-0-470-97608-1, google-Books-ID: 6CstrP_lXQ4C.

Mads M. Pedersen, Alexander Meyer Forsting, P. v. d. L. R. R. L. A. A. R. J. C. R. M. F.-M. J. Q. J. P. S. C. R. V. R. B. T. O. and Réthoré, P.-E.: PyWake 2.5.0: An open-source wind farm simulation tool, https://gitlab.windenergy.dtu.dk/TOPFARM/PyWake, 2023.

Rodrigues, S., Bauer, P., and Bosman, P. A. N.: Multi-objective optimization of wind farm layouts – Complexity, constraint handling and scalability, 65, 587–609, https://doi.org/10.1016/j.rser.2016.07.021.

Saad, D. A., Mansour, H., and Osman, H.: Concurrent bilevel multi-objective optimisation of renewal funding decisions for large-scale infrastructure networks, 14, 594–603, https://doi.org/10.1080/15732479.2017.1378238, publisher: Taylor & Francis _eprint: https://doi.org/10.1080/15732479.2017.1378238.

Saint-Drenan, Y.-M., Besseau, R., Jansen, M., Staffell, I., Troccoli, A., Dubus, L., Schmidt, J., Gruber, K., Simões, S. G., and Heier, S.: A parametric model for wind turbine power curves incorporating environmental conditions, 157, 754–768, https://doi.org/10.1016/j.renene.2020.04.123.

Saravanan, J. and Sridhar, M.: Life cycle assessment of alternative building materials using idematlightlca mobile app, 65, 1243–1249, https://doi.org/10.1016/j.matpr.2022.04.184.

Sorkhabi, S. Y. D., Romero, D. A., Beck, J. C., and Amon, C. H.: Constrained Multi-Objective Wind Farm Layout Optimization: Introducing a Novel Constraint Handling Approach Based on Constraint Programming, in: Volume 2A: 41st Design Automation Conference, p. V02AT03A031, American Society of Mechanical Engineers, ISBN 978-0-7918-5707-6, https://doi.org/10.1115/DETC2015-47535.

Sutherland, H. J.: On the Fatigue Analysis of Wind Turbines, https://doi.org/10.2172/9460.

Tran, R., Wu, J., Denison, C., Ackling, T., Wagner, M., and Neumann, F.: Fast and effective multi-objective optimisation of wind turbine placement, in: Proceedings of the 15th annual conference on Genetic and evolutionary computation, GECCO '13, pp. 1381–1388, Association for Computing Machinery, ISBN 978-1-4503-1963-8, https://doi.org/10.1145/2463372.2463541.

van Heukelum, H., Steenbrink, A., Colomés, O., Binnekamp, R., and Wolfert, A.: Preference-based service life design of floating wind structures, pp. 957–964, ISBN 978-1-00-332302-0, https://doi.org/10.1201/9781003323020-116.

Veeramachaneni, K., Wagner, M., O'Reilly, U.-M., and Neumann, F.: Optimizing energy output and layout costs for large wind farms using particle swarm optimization, pp. 1–7, ISBN 978-1-4673-1510-4, https://doi.org/10.1109/CEC.2012.6253002.